

# DNA melting I: Interplay with counterion condensation

T. Vuletić,\* S. Dolanski Babić,† D. Grgičin, D. Aumiler, and S. Tomić  
*Institut za fiziku, 10000 Zagreb, Croatia*

F. Livolant  
*Laboratoire de Physique des Solides, Université Paris Sud - F-91405 Orsay, France*

J.Rädler  
*Ludwig-Maximilians-Universität, Sektion Physik, Geschwister-Scholl-Platz 1, D-80539 Munich, Germany*  
(Dated: February 24, 2019)

We studied nucleosomal DNA fragments (monodisperse, 146 bp long,  $c = 0.0015 - 8$  mM, in basepair) dilute solutions in very low salt ( $< 0.05$  mM). Conductometry was complemented by fluorescence correlation spectroscopy (FCS) measurements of the DNA polyion diffusion constant  $D_p$ . We found that the normalized solution conductivity  $\sigma/c$  is 50% higher below  $c = 0.05$  mM than above 1 mM.  $\sigma/c$  primarily depends on  $D_p$  and on the charge of the polyion. The observed conductivity crossover must reflect the variation in charge, since  $D_p$  is rather constant in the crossover region, as we established by FCS. Polyion charge depends on the DNA conformation since this charge is renormalized by the Manning condensation of counterions and effectively proportional to the Manning free counterion fraction  $\theta$ . According to Manning, this fraction increases upon DNA denaturation - dsDNA:  $\theta=0.24$ , ssDNA:  $\theta=0.59$ . Experimentally, across the crossover region we extracted a range of values  $\theta = 0.45 \pm 0.02$  to  $\theta = 0.60 \pm 0.03$  or  $\theta = 0.30 \pm 0.02$  to  $\theta = 0.45 \pm 0.03$ , depending whether for the conductivity model the Manning asymmetry field effect is taken into account or not. Thus, conductometry appears as capable as osmometry to quantitatively validate the Manning condensation model.

PACS numbers: Polyelectrolytes 82.35.Rs Transport dynamics of biomolecules, 87.15.hj self-diffusion and ionic conduction in Polymers, 66.30.hk

## I. INTRODUCTION

Stability of the double stranded DNA molecule, of the right-handed double helix in the B-conformation is directly related to the nature of the DNA as a polyelectrolyte [1, 2]. Polyelectrolytes are macromolecules-polymers that, when dissolved in polar solvents dissociate into a polyion and small counterions. Electrostatic interactions and entropy of all those charges, as well as those of added salt control the phenomenology of polyelectrolytes. In the case of DNA the charge distribution, the physics, directly influences the molecular structure, the chemistry. That is, it is rather well established that the stability of dsDNA depends on temperature and on added salt and DNA concentrations [3–5].

The denaturation process is a consequence of the electrostatic interaction of counterions with the polyion. The interaction may be indirect as in the Debye-Hückel screening effect. This effect is reduced at low ionic strength, where there are fewer ions available to redistribute around the negatively charged phosphate groups of the DNA polyion and screen their potential. Effectively, Debye-Hückel screening length becomes large

enough so the phosphate charges on opposite strands "see" each other and their strong Coulombic repulsion tears the hydrogen bonds between DNA bases and thus the double helix apart. Besides the screening effect, electrostatics of the polyelectrolytes feature a strong effect of direct interaction of counterions and the polyion: counterion condensation (Manning condensation) [6]. Strong linear charge of the polyion tends to attract the counterions to its immediate vicinity. The condensation occurs for polyions with the Manning parameter  $u = l_B/b > 1$ , where  $l_B$  is the Bjerrum length, the length at which two elementary charges interact in a given solvent with energy equal to the thermal energy  $kT$  and  $b$  is the average distance between the charges on the polyion backbone. If there is more than one charge per Bjerrum length, the condensation will tend to effectively reduce the linear charge density down to  $1e/l_B$  level. The condensed ions fraction is then equal to  $1 - 1/u$  and the free, uncondensed counterions fraction is  $\theta = 1/u$ . Manning has, however, modeled an infinitely long and thin polyion in pure water, with no added salt, which is a rather unrealistic proposition and not biologically relevant. Nevertheless, the condensation is documented experimentally [13–15] and the theoretical concept may well be extended to higher concentrations of polyelectrolyte and salt [7]. Condensation is also related to the DNA stability: entropic cost to condense or confine the counterions compares with the gain in electrostatic free energy upon DNA denaturation [8]. This gain is due to the single stranded DNA (ssDNA) having a lower linear charge density than dsDNA

---

\*URL: <http://tvuletic.ifs.hr/>; Electronic address: tvuletic@ifs.hr

†Permanent address: Department of physics and biophysics, Medical School, University of Zagreb, 10000 Zagreb, Croatia.

and, according to Manning, the condensed counterions fraction is lower for ssDNA than for dsDNA.

Counterion condensation is most easily experimentally studied and theoretically interpreted for a monodisperse (uniformly sized) and dilute (non-overlapping) solution of rigid, rodlike polyions, which do not change conformation due to condensation. In a dilute solution, effectively, the condensed fraction of counterions may be considered to be found in a cylindrical cell around the polyion, while the rest may be taken to be free inside the spherical volume that belongs to a given polyion [9]. Since the condensed counterions are not chemically bound to the polyion, the free and condensed counterions exchange between the two theoretical regions and only a continuous radial counterion distribution [10] can exist around the polyion, as shown experimentally by EPR (electron paramagnetic resonance) [11]. In other words, there should be no step in the radial counterion distribution which would define the limit of the cylindrical zone. While the theoretical works nominally deal with two types of ions, the experiments also attempt to provide the condensed counterion fraction. This is well justified when one tries to understand the osmotic pressure of a polyelectrolyte [7, 12]. Note that a polyelectrolyte, due to the released counterions has considerably higher osmotic pressure than a neutral polymer of a similar chain size. However, this osmotic pressure appears reduced exactly due to the counterion condensation - only the uncondensed, free counterions contribute. This provides the means for the experimental studies of osmotic pressure of polyelectrolytes to evaluate the free counterions fraction [13–15]. Thus, the concept of two types of counterions gets a physical meaning. This concept also appears naturally in the interpretation of the electrical transport studies of polyelectrolytes, where the condensed counterions are those which, when the electric field is applied, will move together with the polyion, while the free counterions would, due to their opposite charge, move in the opposite way [16]. The experimental studies of transport in polyelectrolytes are again most easily and reliably interpreted for monodisperse dilute solutions [17]. The techniques which may contribute to our knowledge here range from transport measurements like conductometry [18, 19] and capillary electrophoresis [20, 21], to diffusion measurements by dynamic light scattering [20–23] or fluorescence correlation spectroscopy [24, 25]. Manning [26] has proposed a rather comprehensive and convincing conductivity model for polyelectrolytes and Bordi *et al.*[17] worked on including the scaling theories by Rubinstein *et al.*[27], in order to separate the influences from the polyion conformation and charges of polyion and counterions and added salt. Still, one may note that the experimental work has been rather scarce and not very easily compared with theory, at least not in a quantitatively satisfactory manner [28, 29]. For a successful quantitative comparison of the transport experiments with conductivity models one has to use the simplest possible system to study, as well as the experimental method to separate the

influence of charge and the conformation on the transport. One step to this end is to choose a monodisperse dilute polyelectrolyte with no added salt, as the simplest conceivable system. For the convenience of the reader (*cf.* [17]) we will present in the following that the conductivity in the system under study can be understood to be a product of three separate factors characterizing the charge carriers in the system: carrier charge, concentration and their mobility (ratio of carrier velocity and the applied electric field).

$$\sigma = \sum_i z_i n_i \mu_i \quad (1)$$

Index  $i$  denotes different carrier species that present in a solution. That is, in simple electrolytes, the conductivity is a sum of equivalent molar conductances of the ionic species present in solution, multiplied by the charge  $z_i$  and concentration  $c_i$  of the respective ion:

$$\sigma = \sum_i z_i c_i \lambda_i \quad (2)$$

Here, for practical reasons we deal with molar concentrations  $c_i$  and equivalent conductances  $\lambda_i$ , which relate to the mobility via Faraday constant  $F$ :

$$\lambda_i = F \mu_i \quad (3)$$

For polyelectrolytes the expression Eq. 2 stays the same. A monodisperse dilute polyelectrolyte with no added salt solution will contain only two ionic species. However, one ionic species is a macromolecule, a polyion whose contribution to the conductivity is dependent on its size and conformation which influence  $\lambda_p$ . Such a large molecule has a relatively small concentration  $c_p$  and a proportionally large charge  $Z_p$ :

$$\sigma = Z_p c_p \lambda_p + z_i c_i \lambda_i \quad (4)$$

Here we note that  $c_i$  is the concentration of counterions released from the polyelectrolyte upon solvation, which is proportional to the concentration of monomers  $c$  of which the polyion is constituted. The monomer concentration  $c$  is related to the polyion concentration  $c_p$  via:

$$c = N c_p \quad (5)$$

where  $N$  is the polyion degree of the polymerization. Also, the polyion charge is related to the monomer charge  $z_p$ :

$$Z_p = N z_p \quad (6)$$

Due to the electroneutrality of the solution

$$Z_p c_p = z_i c_i = z_p c \quad (7)$$

Thus the conductivity of a polyelectrolyte solution principally depends on the concentration of the monomers  $c$ :

$$\sigma = z_p c (\lambda_p + \lambda_i) \quad (8)$$

Here we remind that the polyion charge is effectively reduced,  $Z_p = \theta N z_p$  due to the counterion condensation, and also that only the free fraction  $\theta c_i$  of counterions may be considered to take part in electrical transport. Therefore:

$$\sigma = \theta z_p c (\lambda_p + \lambda_i) \quad (9)$$

Both experiments [30] and theoretical estimates [17] lead to the conclusion that  $\lambda_i$  of small ions is not significantly changed in polyelectrolytes when compared to values measured in simple electrolytes. Thus to understand the monomer concentration dependence of the measured conductivity, according to Eq.9, one has to distinguish the influence from the charge sector, parametrized by  $\theta$  and from the polyion conformation, parametrized by  $\lambda_p$ . That is,  $\lambda_p$  is defined by the electrophoretic coefficient  $f_E$  of the polyion and its charge  $Z_p$ :

$$\lambda_p = F Z_p / f_E \quad (10)$$

The electrophoretic coefficient primarily depends on the size and shape of the particle, which may be parametrized by its effective hydrodynamic radius  $R_H$ .

$$f_E = 6\pi\eta R_H \quad (11)$$

Here  $\eta$  is viscosity of the medium/solution in which the particle is moving - for dilute solutions this is solvent viscosity. The electrophoretic coefficient is in a simple manner related to the self-diffusion constant of the particle(polyion):

$$D_p = kT / f_E \quad (12)$$

Consequently, the conductivity of a monodisperse polyelectrolyte without added salt is governed by the self-diffusion constant  $D_p$  of its polyion and the free counterion fraction  $\theta$ .

With the goal to quantitate the effects of the diffusion and electrostatics in the charged system of a polyelectrolyte we chose the DNA as a model system. DNA is more readily available as a chain of given size and charge than a synthetic polyelectrolyte, and the preparations may be highly monodisperse.

Therefore we present a study of transport in nucleosomal dsDNA solutions without added salt. Nucleosomal DNA fragments have about 146 bp and are 50 nm long. The crossover concentration for these fragments is  $\approx 2$  mM [31]. As the DNA persistence length is 50 nm [33], similar to the length of the fragments, these are expected to be rather rigid and rod-like. The details of material preparation and experimental methods used are given in Sec. II. In our work, as presented in Sec. III, conductometry (, conductivity measurements) was complemented by fluorescence correlation spectroscopy (FCS) measurements of the DNA polyion self-diffusion constant  $D_p$ . The chosen range of DNA concentrations was 0.0015-8 mM, *i.e.* mostly in the dilute regime [41] to simplify the interpretation of the conductivity and diffusion. Our proposition, discussed in Sec. IV is that upon denaturation, which occurs at ambient temperature only for lower DNA concentrations and without added salt, the equivalent conductivity of the DNA polyion changes due to a change in the counterion condensation. Having both the conductivity and self-diffusion data we are able to present credible values for the free counterions fraction  $\theta$ , comparable to those predicted by Manning, as well as the concentration behaviour of  $\theta$ .

## II. MATERIALS & METHODS

### A. Monodisperse DNA

Large quantities of practically monodisperse 50 nm long nucleosomal DNA fragments were prepared as described in Sikorav *et al.*[34] by enzymatic digestion of calf thymus chromatin, that is, nuclease acting on linker DNA between adjacent nucleosomes [35]. As checked by electrophoresis, the sample contains DNA fragments  $146 \pm 10$ bp long together with traces of 350 bp fragments that correspond to two nucleosomal DNA fragments connected by undigested linker DNA. This DNA will be further denoted DNA146. The samples were stored in dry state, that is, DNA fragments from the preparation solution were precipitated with cold ethanol, centrifuged and the pellets were dried. Low protein content was verified by UV absorption. Our stock, when redissolved did not bring any added salt into the solution. We verified this by a following procedure. A sample from this stock was dissolved at 5 g/L concentration in 10 mM NaCl and then spin-dialyzed against pure water. With spin-dialyzing we mean that the sample was diluted 5 fold with pure water and spin-filtered to the original volume. This procedure was repeated 3 times. Simultaneously, another sample was simply dissolved in pure water. The two samples had similar conductivities (normalized for concentration), and we concluded that neither contained any considerable excess of salt. Any salt that may have been present in the original samples did not raise conductivity more than equivalent of 0.2 Na<sup>+</sup> ions per base pair. We remind, DNA is in the form of Na-salt and it releases

two  $\text{Na}^+$  counterions in the solution. For conductometry and FCS measurements the range of DNA146 solutions  $c_{DNA} = 0.0015 - 8$  mM in pure water was prepared by dilution with pure water of aliquots from the 27mM mother solution. The mother solution was obtained by dissolving 10 mg of dry DNA146 in 0.55 mL pure water.

For FCS measurements the DNA146 solutions were fluorescently labeled by addition of synthetic 110bp dsDNA. This 110bp dsDNA will be further denoted DNA110\* (\* denoting the fluorescent labeling). Synthetic DNA sequences [36] were purchased (Mycrosynth A.G., CH) as two separate oligonucleotides (ssDNA), 110nt long and arrived liophilized. The two sequences were complementary, and only one of them was labeled at one end with covalently bound Cy5 fluorophore. The dry complements were dissolved in 10 mM TE buffer with addition of NaCl up to 60mM. These solutions of complements were mixed and heated to  $97^\circ\text{C}$  for 15 minutes (heating should have removed any hairpin loops previously formed) and then left to cool for several hours, to slowly hybridize and form dsDNA 110 bp long, labeled with Cy5. Hybridization was checked to be complete on the agarose gel. The resulting solution had DNA concentration of 0.5mM in basepair. Respective Cy5 concentration was  $5\mu\text{M}$ . The solution was diluted with 4 times larger volume of 10mM TE buffer and then spin-concentrated to the original volume. The procedure was repeated 3 times to remove excess NaCl.

Prior to FCS measurements in pure water we were adding  $2\mu\text{L}$  of DNA110\* stock into  $500\mu\text{L}$  aliquots of DNA146, of varying concentrations (0.0015-8 mM concentration range) to achieve 20 nM Cy5 label concentration. We note that the DNA146 aliquots, nominally without any added salt or buffer, had a minimal added salt concentration, not above 0.05mM. This is due to 10mM TE buffer of DNA110\* stock which gets 250 times diluted after addition into DNA146 aliquots.

For FCS measurements of DNA146 in buffer, an 0.1 mL aliquot was taken from 27 mM pure water mother solution and diluted with 0.25 mL of 35 mM TE buffer to obtain 7.7 mM DNA146 in 10 mM TE buffer starting solution. For consecutive measurements at lower DNA146 concentrations this solution was further diluted with appropriate volumes of 10 mM TE buffer. On each dilution appropriate volumes of DNA110\* stock were being added to maintain the 20 nM Cy5 level.

For FCS calibration measurements Cy5 fluorophore alone was diluted in pure water to 20 nM.

Traces of liophilized ssDNA [36] that remained in original packaging were washed with 0.3 mL pure water. FCS measurement of this sample provides the value for 110 bases long ssDNA in pure water solution, without DNA146.

Finally, we remind that dsDNA molar concentration (monomolar, basepair concentration) relates with mass concentration with a simple conversion factor 1.5: 1g/L equals 1.5 mM(basepair). These molar concentrations (basepair) will be used in the remainder of the paper.

## B. Fluorescence correlation spectroscopy

Fluorescence correlation spectroscopy inherently probes the system under study both at single molecule and ensemble levels. FCS observes fluorescence intensity fluctuations emitted by fluorescently labeled objects diffusing through a small open volume ( $< 1$  fL) defined by the profile of the laser beam and the optics, objective of the microscope. That is, number fluctuations of the molecules entering and leaving the focal volume are registered as fluorescence variation, which is then recorded and autocorrelated. Thus following practically single molecules we obtain the properties of the ensemble [37, 38]. We have used a commercially available Zeiss ConfoCor II FCS instrument, where the measurement volume was defined by a Zeiss Plan-NeoFluar 100x/NA1.3 water immersion objective, epi-illumination was by He-Ne 632.8 nm 5mW laser, for excitation of Cy5 fluorophore. Zeiss proprietary software was used for autocorrelation function calculation and extraction of diffusion times by non-linear least squares fitting [39]. The physical principles of such an experimental set-up and theoretical background of FCS have been described elsewhere [38, 40], and the manner used to obtain the self-diffusion coefficient of the molecule under study, in our case 110 bp Cy5 labelled dsDNA, is presented in brief in the following. The instrument directly measures fluorescence intensity for *e.g.* 30 seconds. However, of interest is the decay rate of the autocorrelation function  $G(\tau_c)$  calculated for the intensity trace. The decay rate relates to the characteristic time for DNA110\* particle to diffuse through the focal volume. This time reflects the self-diffusion coefficient of fluorescent DNA 110\* molecules. The fluorescence intensity autocorrelation function,  $G(\tau_c)$ , is fitted with a single diffusion time,  $\tau_D$  (inverse of the decay rate) according to

$$G(\tau_c) = \frac{1}{N_f} \cdot \frac{1}{1 + \frac{\tau_c}{\tau_D}} \frac{1}{\sqrt{1 + \left(\frac{w_0}{z_0}\right)^2 \frac{\tau_c}{\tau_D}}} \left(1 + \frac{T}{1 - T} \exp\left(-\frac{\tau_c}{\tau_T}\right)\right) \quad (13)$$

Here  $N_f$  is average number of fluorescent molecules in the confocal detection volume,  $c$  is correlation time. Another fit parameter is  $z_0/w_0$ , the structural factor, *i.e.* the ratio of radial and axial extension of focal volume. The transition of the Cy5 fluorophore to the first excited triplet state and a relatively slow relaxation to ground state influence the observed autocorrelation curve. Thus,  $T$ , average fraction of fluorophores in the triplet state, and  $\tau_T$ , lifetime of the triplet state of the fluorophore are taken into account when fitting. The structure parameter of the volume element  $z_0/w_0 \approx 10$  is obtained from measurements on Cy5 molecules whose diffusion constant is known,  $D_{Cy5} = 3.16 \cdot 10^{-10} \text{ m}^2/\text{s}$  [39]. Thus the structure parameter is not a fit parameter when  $\tau_D$  is being extracted. In Fig.1, we present autocorrelation function experimental curves for  $2\mu\text{M}$  DNA110\* in 0.2 mM DNA146 in buffer and in pure water solution. The dif-

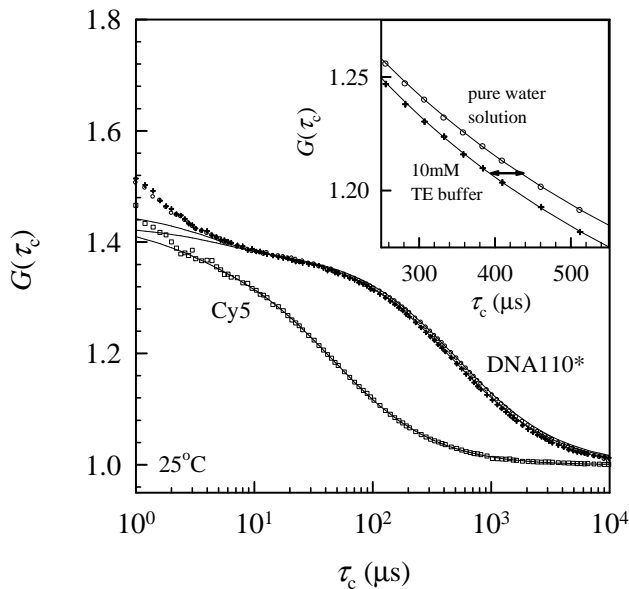


FIG. 1: Experimental autocorrelation functions recorded for 2  $\mu\text{M}$  DNA110\* in 0.2 mM (basepair) DNA146 in 10 mM TE buffer and in pure water solution. The inset demonstrates that the fits to Eq.13 reliably distinguish between the two data sets. The arrow denotes the 40  $\mu\text{s}$  difference between the respective diffusion times obtained by fits. For comparison, the autocorrelation function is shown for 20 nM Cy5 fluorophore in pure water (no DNA). The corresponding diffusion time is about 50  $\mu\text{s}$ .

fusion times  $\tau$ , which are a parameter for fits to Eq.13 are 400 and 440  $\mu\text{s}$ , respectively. The inset demonstrates that the fits reliably distinguish between the two experimental data sets [40].

### C. Conductometry

Dielectric spectroscopy in the range 100Hz-110MHz was performed with Agilent 4294A impedance analyzer. All the measurements were performed at  $25 \pm 0.02^\circ\text{C}$ . Conductometry data was extracted from these spectra. Conductivity was calculated from conductance at 100 kHz and capacitance was read at 10 MHz. Conductivity at 100 kHz shows a minimal influence from the electrode polarization effects, as well as from the conductivity chamber resonance at 100 MHz. Basically, one has to measure a spectrum [41], to be able to confidently extract conductivity values. Only in this manner, the obtained conductivity may be regarded as dc conductivity, the conductivity due to free charges (polyions, counterions, added salt ions). We emphasize that all the conductivities of polyelectrolytes have been deduced for 1.5  $\mu\text{S}/\text{cm}$ , the conductivity of the solvent [42], *i.e.* pure water (Milli-Q, Millipore). This residual conductivity is due to the ambient  $\text{CO}_2$  dissolved in pure water. Consequently, the pH of pure water is about 5.5, however this is unbuffered. The capacitance at 10MHz serves as a check of the

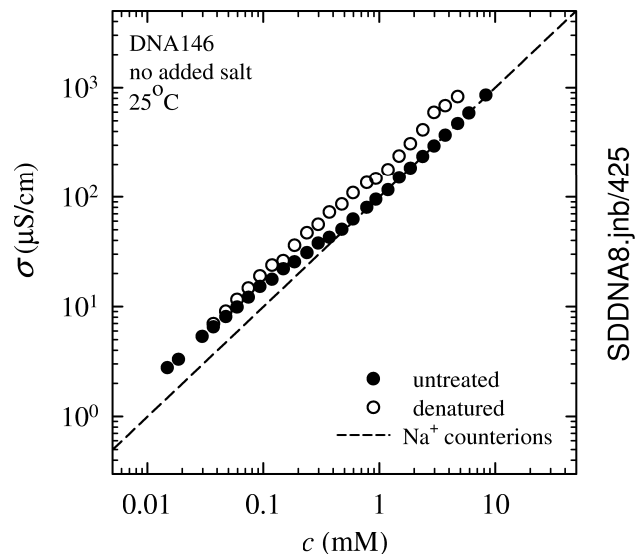


FIG. 2: DNA146 pure water solution conductivity versus DNA base pair concentration. Dashed line represents the conductivity of all the sodium ions nominally present in the solution. Open circles show the conductivity of thermally denatured, *i.e.* heat-treated ( $97^\circ\text{C}$ ) samples, measured at  $25^\circ\text{C}$ . These same samples were also measured prior to the heat-treatment and this data-set (black circles) is denoted untreated.

sample volume for our experimental setup [43]. At this high frequency the contribution to the capacitance comes from the dielectric constant of pure water, and not from the solutes. Thus all the samples should have the same capacitance if they have the same volume.

## III. RESULTS

### A. Electrical transport - free counterions fraction

We present the dc conductivity data for pure water solution of DNA146, nucleosomal 146bp DNA. This conductivity is due to currents originating from the displacement of polyions and counterions as the free carriers in the solution, as there is no polarization current contribution. In this sense the reported values may be regarded as dc values.

Fig.2 emphasizes a general power-law dependence of conductivity on concentration of the pure water DNA146 solution. Denatured samples were prepared by heat treatment of samples previously used for conductivity measurements (denoted untreated, full circles), accomplished by the heating of aliquots for 20 min at a temperature of  $97^\circ\text{C}$ , followed by quenching to  $4^\circ\text{C}$  for a minute and then conductometry at  $25^\circ\text{C}$ . For the denatured samples (open circles) the power law is apparently even better defined. As the conductivity of a polyelectrolyte basically depends on contributions from counterions and polyions, then it is instructive to present the the-

oretical conductivity of all the sodium  $\text{Na}^+$  ions present in solution. Since on the ordinate we present the basepair concentration, there is 2  $\text{Na}^+$  per base pair. *i.e.* for 1 mM base pair DNA sample there will be 2 mM  $\text{Na}^+$  counterions, whose molar conductivity is  $\lambda_{\text{Na}^+} = 50 \mu\text{S}/\text{cm}$ :

$$\sigma_i = 2c\lambda_{\text{Na}^+} \quad (14)$$

This theoretical sodium conductivity is denoted with a dashed line in Fig. 2, and it is apparent that some other ionic species contributes to the conductivity of DNA polyelectrolyte, namely DNA polyions with molar conductivity  $\lambda_p$ , as may be expected from the model for conductivity presented in the Introduction. In this model conductivity contributions have been reduced by the factor  $\theta$ , to account for Manning condensation:

$$\sigma = \theta\sigma_i + 2\theta c\lambda_p = 2\theta c(\lambda_{\text{Na}^+} + \lambda_p) \quad (15)$$

Free counterion fraction  $\theta$  represents the concept (see Introduction) that the condensed counterions do not contribute to the conductivity, and also that they reduce the charge on the polyion and thus polyions' contribution to conductivity. If we normalize the conductivity with concentration, then data may be presented in a physically more relevant form. That is, normalized conductivity concentration dependence is directly related to the behavior of the molar conductivities  $\lambda_{\text{Na}^+}$  and  $\lambda_p$ .

$$\frac{\sigma}{c} = 2\theta(\lambda_{\text{Na}^+} + \lambda_p) \quad (16)$$

In Fig.3 we show this normalized conductivity. We deem that the normalized conductivity (open circles) of the denatured samples is, within the data scatter, constant with value of  $180 \mu\text{S}/\text{cm}$ . On the contrary, the normalized conductivity of the untreated DNA146 samples shows a crossover in the 0.05-1 mM concentration range. Above 1 mM it attains a constant value of  $100 \mu\text{S}/\text{cm}$ , while at the lowest concentration it approaches the  $180 \mu\text{S}/\text{cm}$  value for the heat treated, denatured DNA146 samples. This conductivity crossover has not, to our knowledge, been reported previously, for any DNA sample. The data for denatured samples show a rather high data scatter, which we ascribe to the denaturation procedure. Gradual renaturation, after quenching, and during the measurement at  $25^\circ\text{C}$  was not an issue, as the samples held in our conductivity chamber showed a stable conductivity for at least an hour, and the measurement itself lasted for only 2 minutes. Either denaturation did not proceed to the full extent for all the samples or some of the DNA renatured in hairpins during quenching in some cases [44] and this introduced a conductivity variation. For reference, we have shown with the dashed line the theoretical conductivity of the  $\text{Na}^+$  ions present in the solution (in the same manner as in Fig.2), divided by  $c$ , basepair concentration

$$\sigma_i/c = 2\lambda_{\text{Na}^+} \quad (17)$$

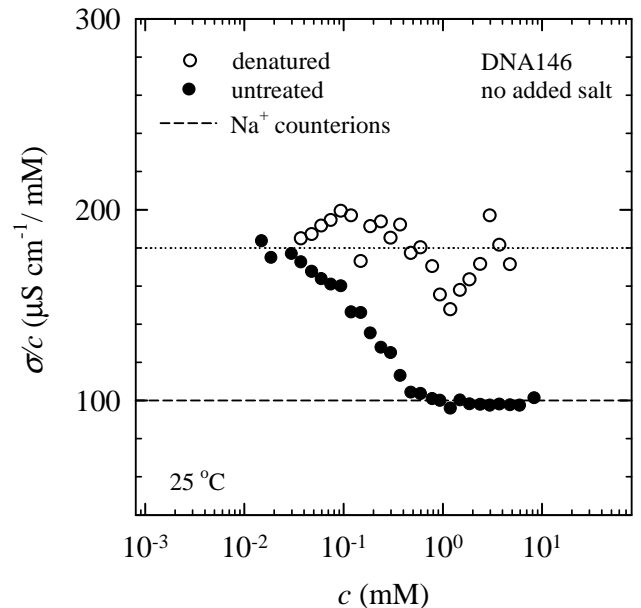


FIG. 3: Untreated and denatured DNA146 conductivities (normalized by concentration) versus DNA concentration (basepairs). The nominal contribution of all the present  $\text{Na}^+$  ions is denoted with a dashed line (see Eq.17) The dotted line shows the average value for denatured samples,  $180 \mu\text{S}/\text{cm}$ . The values for untreated samples also approach this value.

## B. Polyion diffusion

We have experimentally obtained the diffusion coefficient  $D_p$  of the DNA146 polyion by adding fluorescently labeled dsDNA, DNA110\*, up to  $2 \mu\text{M}$ , into DNA146 samples of varying concentrations (0.0015-8 mM, basepair). Sets of DNA146 samples have been prepared both in pure water and in 10 mM TE buffer. DNA in the buffer is used as a control, as it will positively keep the native conformation.

The labeled DNA is thus somewhat shorter than the bulk of DNA in the sample solution. However both DNA110\* and DNA146 consist of short fragments, 38 and 50 nm in length, respectively, which is comparable to dsDNA persistence length. Consequently, both molecules could be regarded as rigid rods (cylinders) and in principle it should be possible to rescale the diffusion coefficient obtained for one of them, *i.e.* DNA110\* and get the value for the other, DNA146. In this manner, fluorescence correlation spectroscopy was used to obtain the self-diffusion coefficient of DNA146 at varying concentrations (0.0015-8 mM, basepair).

Fits to the fluorescence intensity autocorrelation function, Eq.13 provide the diffusion time. This is the time a fluorescently labeled molecule takes to traverse the focal volume. It is inversely proportional to the molecules' diffusion coefficient. Measurements of the diffusion time for Cy5 fluorophore molecule alone, whose diffusion coefficient is known, provide means for conversion of the diffusion times measured for other molecules also. Thus,

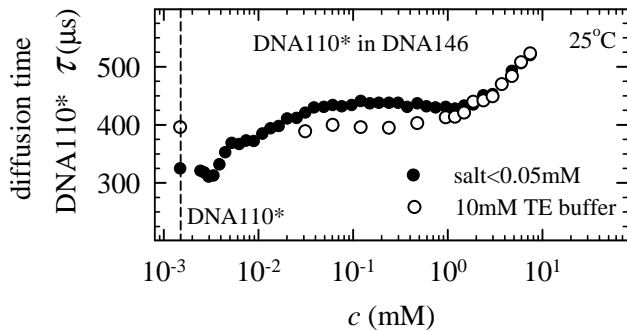


FIG. 4: Fluorescently labeled 110 bp dsDNA (DNA110\*), was added to 2  $\mu\text{M}$  into samples of varying DNA146 concentrations. DNA110\* diffusion time measured by fluorescence correlation spectroscopy (FCS) is shown versus combined DNA110\*+DNA146 concentration  $c$  (basepairs). Full points denote pure water DNA146 solutions while the open points denote DNA146 prepared in 10 mM TE buffer. The dashed line denotes the diffusion time values  $\tau_{110*}^{ss}$  for a sample of the original ssDNA 110 nt oligo in pure water, and also for a sample of double-stranded DNA110\*  $\tau_{110*}^{ds}$ , measured in a buffer. Both were measured without any DNA146 in solution.

a diffusion coefficient  $D$  is obtained from the measured diffusion time  $\tau$  (see Fig.4) by using the following equation

$$D = D_{Cy5} \frac{\tau_{Cy5}}{\tau} \quad (18)$$

where  $D_{Cy5}$  is  $D_{Cy5} = 31.6 \cdot 10^{-11} \text{ m}^2/\text{s}$  [39] and  $\tau_{Cy5}$  we have measured to be  $50 \pm 2 \mu\text{s}$ .

### 1. Rod-like diffusion

We note that the diffusion time for DNA110\* in the buffer is constant below about 1 mM:  $\tau = 400\mu\text{s}$ . Inserting into Eq. 18 we get the diffusion coefficient for DNA110\*:  $D_{110*}^{exp} = 3.95 \cdot 10^{-11} \text{ m}^2/\text{s}$ . This value is very close to the values found by Mandelkern *et al.*[22] by dynamic light scattering or the values one can read from Fig.2 in the work by Stellwagen *et al.*[21] on dsDNA. This diffusion coefficient is also very close to the theoretical value, which can be calculated starting from the concept that short DNA fragments diffuse as rigid rods. That is, DNA110\* and DNA 146, 38 and 50 nm long, respectively, have lengths comparable to the dsDNA persistence length  $L_p = 50 \text{ nm}$ . Therefore, an extended rod-like configuration might be expected, especially at low salt conditions. According to Tirado *et al.*[20] the translational diffusion coefficient calculated for a rod-like macromolecule is given by

$$D^{th} = \frac{kT}{3\pi\eta} \frac{\ln(L_c/d) + 0.312}{L_c} \quad (19)$$

Here  $L_c = Nb$  is contour length,  $d$  is polyion diameter,  $\eta = 8.9 \cdot 10^{-4} \text{ Pas}$  is viscosity of water ( $T = 25^\circ\text{C}$ ). With

$b = 0.34 \text{ nm}$  and  $d = 2.6 \text{ nm}$ , the diffusion coefficient of 110bp DNA is  $D_{110*}^{th} = 3.98 \cdot 10^{-11} \text{ m}^2/\text{s}$ . Stellwagen *et al.*[21] have reviewed the literature and shown that this expression is well applicable for experimental data for DNA molecules in size from 10 to 1000 basepairs. In conclusion, we consider that our FCS measurements are a reliable method to obtain the diffusion coefficients  $D$  of short DNA polyions from the measured diffusion times  $\tau$ .

### 2. DNA146 diffusion coefficient

The diffusion coefficients for DNA110\* that we can obtain from the FCS measured diffusion times should be converted into the diffusion coefficient for DNA146,  $D_{146}$ . This is necessary since we have to use  $D_{146}$  in conjunction with the electrical transport data (see previous section 3.2). Since Eq. 19 is broadly applicable, we will use it to extrapolate  $D_{110*}^{exp}$  to get the value of the diffusion coefficient for 146bp DNA,  $D_{146}^{exp}$ . That is, the relationship which holds between the theoretical values should also hold for the experimental values. Thus,

$$D_{146}^{exp} = \frac{D_{146}^{th}}{D_{110*}^{th}} D_{110*}^{exp} \quad (20)$$

Using Eq.19 to get  $D_{146}^{th}$  and  $D_{110*}^{th}$  and Eq.18 to get  $D_{110*}^{exp}$  from the diffusion times  $\tau_{110*}$  for DNA110\*, we directly convert  $\tau_{110*}$  into the diffusion coefficients for DNA146,  $D_{146}^{exp}$ . For example, for DNA146, in TE buffer (thus, in the native conformation), at low DNA concentrations below 1 mM(basepairs) we get  $D_{146}^{exp} = 3.2 \cdot 10^{-11} \text{ m}^2/\text{s}$ , which is practically equal to the theoretical value  $D_{146}^{th} = 3.27 \cdot 10^{-11} \text{ m}^2/\text{s}$  that we get from Eq.19.

## IV. DISCUSSION

### A. Manning free counterions fraction $\theta$

We have shown in the Introduction how the polyelectrolyte conductivity, as well as the polyion conductivity should relate to the counterion condensation. DNA melting would certainly influence condensation process reflecting in the change of the free counterion fraction  $\theta$ . Theoretically,  $\theta$  should strongly increase upon DNA denaturation/melting. For dsDNA  $\theta = 0.24$  while for ssDNA it reaches 0.59, since the Manning parameter for dsDNA is  $u = 4.2$  and for ssDNA  $u = 1.7$ . Such an increase in  $\theta$  should lead to an increase in the polyelectrolyte conductivity, see Eq.15. Osmometry for dsDNA [13–15] has insofar been the primary experimental source of  $\theta$  data of sufficient quality to devise extensions to Manning theory [7]. Conductometry has been performed on different synthetic polymers, and has insofar given results for  $\theta$  which only agree with Manning within a prefactor of the order of unity [18, 19, 28, 29, 45]. We identify as the main

issues that these experiments were either performed in semi-dilute solutions or with polydisperse samples and, most importantly, the synthetic polymers used were usually rather flexible. In these cases the conformation of the polyion is not well defined and renders analysis difficult due to the necessity to introduce a model for the conformation, besides the model for condensation and conductivity. However, modeling conformation of a flexible polyion in varying salt and monomer concentration is an elaborate problem in itself [17, 27]. On the contrary, our DNA146 sample in buffer has well defined and simple rod-like conformation, and is dilute and highly monodisperse. It is also distinct by the fact that it changes conformation through DNA melting transition in a rather well understood manner.

DNA polyion molar conductivity is influenced by variation of  $D_p$ , the polyion self-diffusion coefficient. In general,  $D_p$  depends on the size and shape of the molecule - in this case on the DNA conformation - which certainly changes upon denaturation:

$$\lambda_p = FZ_p \frac{D_p}{kT} \quad (21)$$

here  $Z_p$  is the polyion charge equal to  $2\theta Ne$ , where  $N$  is the degree of polymerization (number of basepairs for dsDNA, nucleotides for ssDNA),  $F$  is the Faraday constant,  $e$  is unit charge,  $kT$  is Boltzmann energy. We get:

$$\lambda_p = 2\theta N D_p \frac{Fe}{kT} \quad (22)$$

A factor of 2 is present since there are two  $\text{Na}^+$  ions and two negative charges (phosphate) found on one base pair in native dsDNA, as well as there are two  $\text{Na}^+$  ions found on two separate nucleotides on two separate strands. Note that  $\theta$  enters both in the polyelectrolyte conductivity Eq.16 and again in molar conductivity of the polyion Eq.22. In other words, conductometry convolutes the influence of counterion condensation and the DNA conformations, since molar conductivity is a function of both,  $\lambda_p \propto \theta \cdot D_p$ . Then, inserting Eq.22 into Eq.16 we get a quadratic equation for  $\theta(c)$  as a variable and  $D_p(c)$  and  $\sigma(c)$  as the parameters:

$$\theta(c)^2 + \frac{\lambda_{\text{Na}^+}}{D_p(c) \cdot cte.} \theta(c) - \quad (23)$$

$$-\frac{\sigma(c)}{c} \frac{1}{2D_p(c) \cdot cte.} = 0 \quad (24)$$

Here *cte.* stands for a product of several constants (defined previously):  $2NF_e/kT$ . Our measurements of the DNA146 polyelectrolyte conductivity  $\sigma(c)$  and our independent probe of DNA146 diffusion coefficient  $D_p(c) = D_{146}^{exp}$  allow for the equation to be solved for the free counterion fraction  $\theta$ , without a necessity to model the DNA conformation through the melting transition. The equation is to be solved repeatedly for each concentration  $c$ ,

resulting in a concentration dependence  $\theta(c)$ . We take only the positive solutions as the physically meaningful. The concentration dependence  $\theta(c)$ , according to Eq.24 for 146bp nucleosomal DNA (DNA146) in pure water is shown (full points) in Fig.5. At lower concentrations  $\theta$  reaches a value  $\theta = 0.45 \pm 0.03$ . Above 0.05 mM, in the concentration region B, it starts to decrease, and above about 1 mM, in the concentration region A, it is constant at  $\theta = 0.30 \pm 0.02$ . It is apparent that the range of values for  $\theta$  falls nicely within the range that may be calculated for DNA according to Manning theory of counterion condensation [6].

While the crossover in  $\theta$  correlates with the DNA conformational changes across the studied concentration range we note that the exact  $\theta$  values may depend on the details and corrections to the simplest conductivity model we used. Manning has provided a conductivity model, which takes into account *asymmetry field* effect, due to the distortion of the ionic atmosphere surrounding the polyion, occurring when the polyion is subjected to an external electric field [26]. The original work by Manning was reviewed and presented by Bordi *et al.*[18] in the form easily applicable here. Asymmetry field effect corrects  $\theta$  by a factor  $B = 0.866$  for the difference in the diffusion coefficients of counterions in the limit of infinite dilution and in the presence of polyions. Asymmetry field influences the effective observable molar conductivity of the polyion, again through the factor  $B$ :

$$\lambda'_p = 2\theta B N D'_p \frac{Fe}{kT} \quad (25)$$

The diffusion constant  $D_p(c) = D_{146}^{exp}$  we have experimentally obtained in free diffusion, without electric field. The model requires for it to be renormalized:

$$D'_p = D_p \frac{1}{1 + N \frac{D_p}{D_{\text{Na}^+}} \cdot 2\theta B \frac{1-B}{B}} \quad (26)$$

Here  $D_{\text{Na}^+}$  is the diffusion coefficient of free Na ions in simple, dilute electrolyte,  $1.33 \cdot 10^{-9} \text{m}^2/\text{s}$ . Considering the above, the Eq. 16 becomes

$$\frac{\sigma}{c} = 2\theta B (\lambda_{\text{Na}^+} + \lambda'_p) \quad (27)$$

Inserting the Eqs. 25 and 26 into Eq. 27 we get another equation to obtain the free counterion fraction:

$$\frac{\sigma}{c \lambda_{\text{Na}^+}} = 2\theta B \cdot \left( 1 + 2\theta B N \frac{D_p}{D_{\text{Na}^+}} \frac{1}{1 + N \frac{D_p}{D_{\text{Na}^+}} \cdot \frac{1-B}{B} \cdot 2\theta B} \right) \quad (28)$$

In analogy with Eq.24, we rewrite this into a quadratic equation where we only take the positive, physical solution:

$$1/B M x(c)^2 + (1 - AM \frac{1-B}{B}) x(c) - \frac{\sigma}{c \lambda_{\text{Na}^+}} = 0 \quad (29)$$

Here  $M$  stands for  $N \frac{D_p}{D_{Na^+}}$  and  $A$  stands for  $\frac{\sigma}{c\lambda_{Na^+}}$ . Open points in Fig.5 show the asymmetry field corrected  $\theta'(c) = x(c)/2B$ . Overall behaviour of  $\theta'(c)$  is analogous to  $\theta(c)$  behaviour calculated with Eq.24, with a crossover in the concentration region B, and the relative change of  $\theta$  in the crossover region remains about 50%. However, the range of values is different. At low concentrations  $\theta'(c) = 0.60 \pm 0.03$  reaches the theoretical value for ssDNA  $\theta = 0.59$ , while at high concentrations it decreases only down to  $\theta = 0.4 \pm 0.02$ .

Notwithstanding the conductivity model, the obtained  $\theta$  values which correspond to Manning model predictions both for ssDNA and dsDNA corroborate and complement the unique result by Auer and Aleksandrowitz [13] obtained by osmometry. They obtained  $\theta = 0.3$  for semidilute DNA solutions in the concentration range 2-10 mM (basepair). Beyond immediate confirmation of Mannings concepts this similarity in values draws our final remark. Both the transport techniques and osmometry experimentally differentiate the counterions into free and condensed, in two functionally separate populations. The transport identifies as free counterions those that do not move with the polyion in the external electric field. In other words, the free counterions are those that are not close to the polyion, not condensed. However, they may still be within the reach of the polyion potential, as their polarization response is detected by dielectric spectroscopy [46]. Osmometry identifies as free the counterion fraction that contributes to the osmotic pressure of the solution. That is, the counterions that diffuse as free particles, presumably at distance from the polyion and it's potential. Thus defined, the two groups are not necessarily the same, however, this appears to be the case, within the experimental error.

## V. SUMMARY AND CONCLUSION

In this work we have addressed the interplay of the DNA melting (denaturation) transition and the counterion condensation in very low salt ( $< 0.05$  mM) solutions. We used nucleosomal DNA fragments (monodisperse, 146 bp long,  $c = 0.0015 - 8$  mM, in basepair) in dilute solution. First, our conductometry study revealed that the DNA solution molar conductivity normalized by DNA concentration, attains 50% higher value below 0.05 mM than above 1 mM (basepair). The results for solutions of ssDNA (actually, samples of thermally denatured dsDNA) lacked this conductivity crossover. The origin for this conductivity crossover we found in the increase of free charge fraction and decrease in counterion condensation on the polyion, that occurs with DNA denaturation. That is, gradually, at consecutively lower concentrations DNA becomes more denatured. Application of fluorescence correlation spectroscopy (FCS) allowed to quantify the free counterions fraction  $\theta$  which is a function of normalized conductivity and the diffusion coefficient of DNA polyion  $D_p$ . Variations in DNA conformation

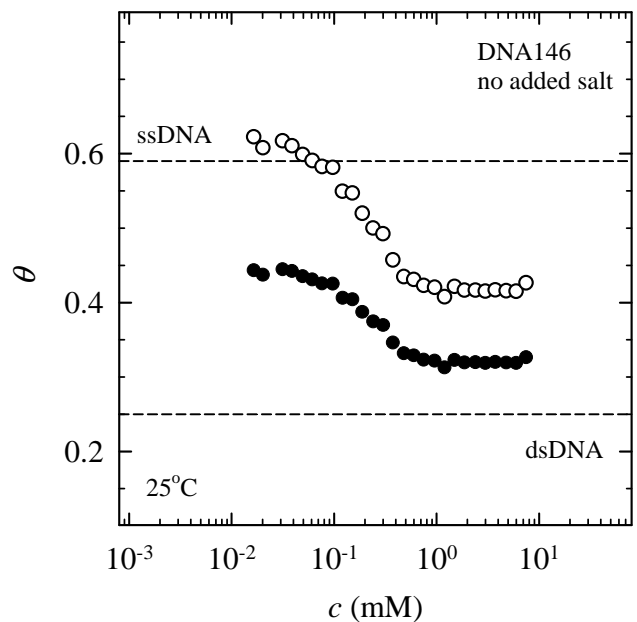


FIG. 5: Free counterion fraction  $\theta$  for 146bp nucleosomal DNA (DNA146) in pure water versus the DNA concentration  $c$  (in mM basepairs). Full points denote  $\theta(c)$  calculated according to the simplest conductivity model, see Eq.16. Open points denote the results from a conductivity model where asymmetry field effect was taken into account to calculate  $\theta'(c)$ . Dashed lines denote the theoretical value of  $\theta = 0.24$  for dsDNA and  $\theta = 0.59$  for ssDNA, as labeled.

due to denaturation appear to be of lesser influence on the polyion conductivity than the DNA polyion effective charge variation. Depending if the asymmetry field effect was taken into conductivity model we obtained the values within the ranges  $\theta = 0.40 \pm 0.02$  to  $0.60 \pm 0.03$  or  $\theta = 0.30 \pm 0.02$  to  $0.45 \pm 0.03$ , respectively. These values confirm and complement the values obtained in osmometry studies by other authors. It appears that osmometry and conductometry detect quite similar counterions populations as the free counterions, as they get quite similar  $\theta$  values. All these quantitatively validate Manning condensation concept. Theoretically, for ssDNA free counterion fraction is  $\theta = 0.59$  and for dsDNA  $\theta = 0.24$ . Further application of FCS, with samples subjected to an external electric field (similar as used for conductometry) could quantitate asymmetry field effect on the diffusion coefficient of DNA146 polyion and reveal to what extent the condensed counterions move with the polyion. Finally, combined conductometry and FCS studies of dilute monodisperse DNA in added salt solutions could extend the studies of  $\theta$  and further complement the data obtained by osmometry.

## Acknowledgement

We gratefully acknowledge A.S. Smith and R. Podgornik for illuminating discussions. This work is based

on the support from the Unity through Knowledge Fund, Croatia under Grant 22/08. The work was in part funded by IntElBioMat ESF activity. The group at the Institute

of physics works within Project No. 035-0000000-2836 of Croatian Ministry of Science, Education and Sports.

- 
- [1] M. Rubinstein, R. H. Colby *Polymer Physics Oxford University Press, USA* (2003); J. R. C. van der Maarel *Introduction to Biopolymer Physics World Scientific, Singapore* (2007)
- [2] V. A. Bloomfield, D. M. Crothers and I. Tinocco, Jr., *Nucleic Acids* (University Science Books, Sausalito, 2000).
- [3] M. T. Record, Jr., *Biopolymers* **14**, 2137 (1975).
- [4] Y. Z. Chen, and E. W. Prohofsky, *Phys. Rev. E* **48**, 3099 (1993).
- [5] T. Dauxois, M. Peyrard, and A. R. Bishop, *Phys. Rev. E* **47**, 684 (1993).
- [6] G. S. Manning, *J. Chem. Phys.* **51**, 924 (1969)
- [7] P. L. Hansen, R. Podgornik and V. A. Parsegian, *Phys. Rev. E* **64**, 021907 (2001).
- [8] G. S. Manning, *Biopolymers* **11**, 937-949 (1972)
- [9] A. Deshkovski, S. Obukhov, and M. Rubinstein, *Phys. Rev. Lett.* **86**, 2341 (2001).
- [10] M. Le Bret and B. H. Zimm, *Biopolymers* **23**, 271 (1984)
- [11] D. Hinderberger, H. W. Spiess, G. Jeschke, Radial Counterion Distributions in Polyelectrolyte Solutions Determined by EPR Spectroscopy, *Europhys. Lett.* **70**, 102-108 (2005)
- [12] D. Antypov and C. Holm, *Phys. Rev. Lett.* **96**, 088302 (2006); D. Antypov and C. Holm, *Macromol. Symp.*, **245-246**, 297-306 (2006).
- [13] H. E. Auer and Z. Alexandrowicz, *Biopolymers* **8**, 1 (1969).
- [14] E. Raspaud, M. da Conceicao and F. Livolant, *Phys. Rev. Lett.* **84**, 2533 (2000).
- [15] R. Podgornik, D. C. Rau, and V. A. Parsegian, *Macromolecules* **22**, 1780 (1989); H. H. Strey, V. A. Parsegian, and R. Podgornik, *Phys. Rev. E* **59**, 999 (1999).
- [16] S. Fischer, A. Naji, R. Netz, *Phys. Rev. Lett.* **101**, 176103 (2008).
- [17] F. Bordi, C. Cametti, T. Gili, *Phys. Rev. E* **66**, 021803 (2002).
- [18] F. Bordi, C. Cametti, and R. H. Colby, *J. Phys.: Condens. Matter* **16**, R1423 (2004).
- [19] D. Truzzolillo, F. Bordi, C. Cametti, and S. Sennato, *Phys. Rev. E* **79**, 011804 (2009)
- [20] M. Mercedes Tirado, C. Lopez Martinez, J. Garcia de la Torre, *J. Chem. Phys.* **81**, 2047-2051 (1984).
- [21] E. Stellwagen, Y. Lu, N. C. Stellwagen, *Biochemistry* **42**, 11745-11750 (2003).
- [22] M. Mandelkern, J. G. Elias, D. Eden and D. M. Crothers *J. Mol. Biol.* **152**, 153-161 (1981).
- [23] R. Pecora, *Macromol. Symp.*, **229**, 18-23 (2005).
- [24] A. Wilk, J. Gapinski, A. Patkowski, R. Pecora, *J. Chem. Phys.* **121**, 10794 (2004).
- [25] S. T. Hess, S. Huang, A. A. Heikal, W. W. Webb, *Biochemistry* **41**, 697-705 (2002)
- [26] G. S. Manning, *J. Phys. Chem.* **85**, 1506 (1981).
- [27] A. V. Dobrynin and M. Rubinstein, *Prog. Polym. Sci.* **30**, 1049 (2005); A. V. Dobrynin, R. H. Colby and M. Rubinstein, *Macromolecules* **28**, 1859 (1995).
- [28] C. Wandrey, *Langmuir* **15**, 4069-4075 (1999).
- [29] C. Wandrey, D. Hunkeler, U. Wendler, and W. Jaeger, *Macromol.* **33**, 7136-7143 (2000).
- [30] T. E. Angelini, R. Golestanian, R. H. Coridan, J. C. Butler, A. Beraud, M. Krisch, H. Sinn, K. S. Schweizer and G. C. L. Wong, *Proc. Natl. Acad. Sci. USA* **103**, 7962 (2006).
- [31] P. G. de Gennes, P. Pincus, R. M. Velasco, and F. Brochard, *J. Phys. (Paris)* **37**, 1461 (1976).
- [32] M. Muthukumar, *J. Chem. Phys.* **105**, 5183 (1996).
- [33] C. G. Baumann, S. B. Smith, V. A. Bloomfield and C. Bustamante, *Proc. Natl. Acad. Sci. USA* **94**, 6185 (1997).
- [34] J. L. Sikorav., J. Pelta F. Livolant, *Biophys. J.*, **67**, 1387 (1994).
- [35] T. E. Strzelecka and R. L. Rill, *J. Am. Chem. Soc.* **109**, 4513-4518 (1987).
- [36] Custom oligonucleotides 110 bases long, with complementary sequences as specified. Synthesis scale was 0.2  $\mu$ mol with PAGE purification step. Cy5 fluorophore was covalently bound to 5' end of Sequence 2. Sequence 1 (5'-3'): GAA GGA GCG GCC AGA GAT TTC TCT TCC TTC AGA TTT TGA GCA TAC AAT TCA TGT TGG TTT TGA TGC TGT CAC AGG GGA GTT TAC GGG GAT GCC AGA ACA GTG GGC CCG CT  
Sequence 2 (5'-3'): AGC GGG CCC ACT GTT CTG GCA TCC CCG TAA ACT CCC CTG TGA CAG CAT CAA AAC CAA CAT GAA TTG TAT GCT CAA AAT CTG AAG GAA GAG AAA TCT CTG GCC GCT CCT TC
- [37] R. Rigler, Ü. mets, J. Widengren, and P. Kask, *Eur. Biophys. J.* **22**, 169-175 (1993).
- [38] P. Schwille, J. Bieschke, F. Oehlenschlager, *Biophys. Chem.* **66**, 211-228 (1997).
- [39] Carl Zeiss: Applications Manual LSM 510 - ConfoCor 2 Application Handbook
- [40] S. Manganot, S. Keller and J. Rädler, *Biophys. J.* **85**, 1817-1825 (2003).
- [41] S. Tomić, S. Dolanski Babić, T. Ivek, T. Vuletić, S. Krča, F. Livolant, and R. Podgornik, *Europhys. Lett.* **81**, 68003 (2008).
- [42] We note that in the work by Truzzolillo *et al.* [19] it appears that the authors have not removed the residual conductivity (about 5-15  $\mu$ S/cm in their case) which seriously influenced their analysis.
- [43] T. Vuletić, S. Dolanski Babić, T. Ivek, D. Grgičin, S. Tomić, and R. Podgornik, *Phys. Rev. E* **82**, 011922 (2010).
- [44] A. Montrichok, G. Gruner and G. Zocchi, *Europhys. Lett.* **62**, 4528 (2003).
- [45] F. Bordi, C. Cametti, A. Motta, and G. Paradossi, *J. Phys. Chem. B* **103**, 5092-5099 (1999).
- [46] S. Tomić, S. Dolanski Babić, T. Vuletić, S. Krča, D. Ivanković, L. Griparić and R. Podgornik, *Phys. Rev. E* **75**, 021905 (2007).
- [47] D. Baigl and K. Yoshikawa, *Biophys. J.* **88**, 3486-3493 (2005).

- [48] D. Poland and H. A. Scheraga, *J. Chem. Phys.*, **45**, 1456; **45**, 1464 (1966).
- [49] E. Carlon, E. Orlandini, A. L. Stella, *Phys. Rev. Lett.*, **88**, 198101 (2002).
- [50] Y. Kafri, D. Mukamel and L. Peliti, *Phys. Rev. Lett.*, **85**, 4988 (2000).
- [51] G. Altan-Bonnet, A. Libchaber, and O. Krichevsky, *Phys. Rev. Lett.*, **90**, 138101 (2003).